Journal of Physics: Conference Series **628** (2015) 012095 doi:10.1088/1742-6596/628/1/012095

Damage localization in a glass fiber reinforced composite plate via the surface interpolation method

M P Limongelli [1], **V Carvelli**[2]
[1,2]Politecnico di Milano, Department of Architecture, Built Environment and Construction Engineering, Milano, Italy.

E-mail: mariagiuseppina.limongelli@polimi.it

Abstract. This work deals with the application to composite plates of the surface interpolation method (SIM) for damage localization. The procedure, which is a generalization to the two-dimensional case of the previously published Interpolation Damage Detection Method (IDDM), locates reductions of stiffness in two-dimensional structures such as plates. The method is based on the damage sensitive of a spline function accuracy in fitting the operational displacement shapes, relies on the so-called Gibbs' phenomenon for splines. This phenomenon occurs when a spline function interpolates discontinuous functions and consists in sharp oscillations and overshoots (values higher than those of the function to be interpolated) near a discontinuous point. The operational deformed shapes are recovered from frequency response functions (FRF's) measured at different locations of the structure during vibrations. The accuracy of the spline interpolation is measured by an error function defined as the difference between the measured and interpolated operational deformed shapes. At a certain location an increase (statistically meaningful) of the interpolation error, with respect to a reference configuration, points out a localized variation of the operational shapes thus revealing the existence of damage. The accuracy of the surface interpolation method is experimentally assessed by impact hammer tests on glass fiber/vinylester composite plates progressively damaged and using finite element numerical modelling.

1. Introduction

Plates are important structural elements, widely used in several engineering applications and the monitoring of their condition is an important aspect for the assessment of the global structural condition. Damage detection techniques traditionally consist in visual inspection and/or non-destructive testing (acoustic, ultrasonic, magnetic field, thermal field methods). A different approach consists in vibration based methods detecting changes of feature related to damage. In the last twenty years several features have been proposed in literature; some of these rely on modal frequencies and/or shapes or their derivatives. In reference [1] a comprehensive state of the art of modal methods is reported.

One drawback of modal methods is related to the need of estimating modal parameters introducing error related to experimental noise that sometime hampers a correct identification of damage. This makes more feasible, approaches based on the use of operational deformed shapes [2]-[4]. The first

[1] corresponding author

author of this paper recently proposed the Interpolation Damage Detection Method (IDDM) for beam-like structures [4], [5] and [6]. The focus of this paper is on the extension of the IDDM to plates. In the following, after a brief overview of the method, the results of experimental tests carried out on a glass fiber reinforced composite plate in the undamaged and in a damaged configuration are reported.
The outline of the paper is as follows. In section 2, the interpolation via bi-cubic spline functions is briefly described and the Gibbs phenomenon for splines is presented and discussed with reference to a simple case. In section 3 the extension of the Surface Interpolation Method is presented and in section 4 the results of experimental tests carried out on a glass fiber reinforced composite plate are detailed.

2. The surface interpolation damage detection method

2.1. Bicubic spline interpolation

A bi-cubic spline interpolation can be used to interpolate an $F(x, y)$ with a smooth surface, which is a function that guarantees continuity of first and second derivatives.
A bi-cubic spline can be thought as a surface constructed from families of cubic spline functions.
Given the values of a function $F(x, y)$ defined on a rectangular grid of $n_{l+2} \times n_{p+2}$ nodes, consider the following equation:

$$s(x,y):\ s_p(x,y)=\sum_{j=0}^{3} c_{jp}(x)(y-y_p)^j \qquad y\in[y_p, y_{p+1}] \qquad \text{with } p=0, 2..., n_p \tag{1}$$

For each value of x, equation (1) gives a spline function along y (see black curves in Figure 1). When x varies, the coefficients $c_{jp}(x)$ also vary and a family of cubic spline functions $s(x,y)$ is obtained.

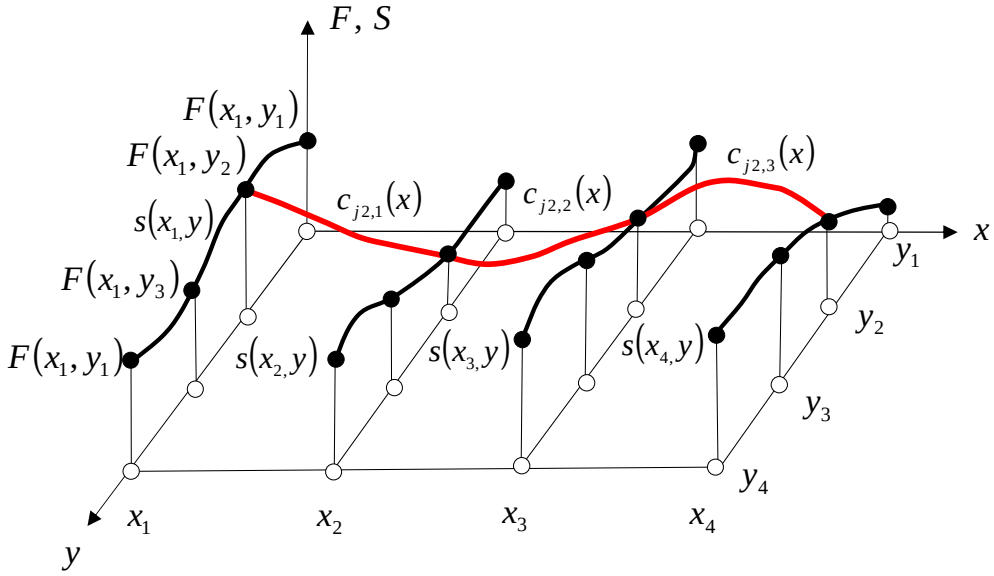

Figure 1. Bi-cubic spline interpolation.

If also the coefficients $c_{jp}(x)$ are defined by cubic spline functions (see red line in Figure 1) in each sub-area defined by $x\in[x_l, x_{l+1}];\ y\in[y_p, y_{p+1}]$ they can be written as:

$$c_{jp}(x): \qquad c_{jp,l}(x)=\sum_{i=0}^{3} a_{jp,il}(x-x_l)^i \qquad x\in[x_l, x_{l+1}];\ y\in[y_p, y_{p+1}]; \tag{2}$$

p=0, 2..., n_p *and* l=0, 2..., n_l
In this case, the following function $S(x,y)$ is a bi-cubic spline function defined through its restrictions to sub-areas as:

$$S(x,y): \qquad S_{l,p}(x,y)=\sum_{j=0}^{3}\sum_{i=0}^{3} a_{jp,il}(x-x_l)^i(y-y_p)^j \qquad x\in[x_l, x_{l+1}];\ y\in[y_p, y_{p+1}] \tag{3}$$

The coefficients $a_{jp,il}$ of the bi-cubic spline function are calculated knowing the function $F(x,l)$ at the nodes and, once the coefficients $a_{jp,ol}$ are known, the bi-cubic interpolation can be finally calculated using equation (3).

2.2. The Gibbs phenomenon for cubic splines

The Interpolation Method is based on the assumption of a beam-like behavior of the monitored structure and on the interpolation of the operational displacement shapes via a cubic spline function.

The process of interpolation consists in recovering continuous data from a discrete set of data, basing on a given model; this is a fundamental operation in several fields were resampling of a limited set of data is needed. For example, image processing may be used when there is the need to reconstruct the data lost in a previous image sampling process in order to change the size of images and/or to correct spatial distortions. Cubic Spline functions in image resampling are widespread used because they are the smoothest among all the functions that interpolate a given set of data and they are stable. Furthermore the cubic spline interpolating functions have a local character, that is a steep variation of the data in a small interval affects only locally the interpolating function. For these reasons cubic spline interpolation are capable of providing high accuracy at a low computational cost which makes them a good choice in case smooth transitions between sampled data are required.

On the other hand the high smoothness of the spline function may be a drawback for a reliable interpolation in case of non-smooth regions of curves. This is due to a phenomenon known as '*Gibbs' phenomenon of splines*' occurring when the spline interpolates functions with discontinuities: the spline interpolation oscillates near a discontinuous point and has an overshoot (values higher than those of the function to be interpolated[7]). In Figure 2 this phenomenon is illustrated with reference to a continuous (C^1) function $f(x)$ with a jump of curvature at section x=1: the cubic spline interpolation $s(x)$ of the function exhibits strong oscillation around the actual value of the function (see Figure 2a).

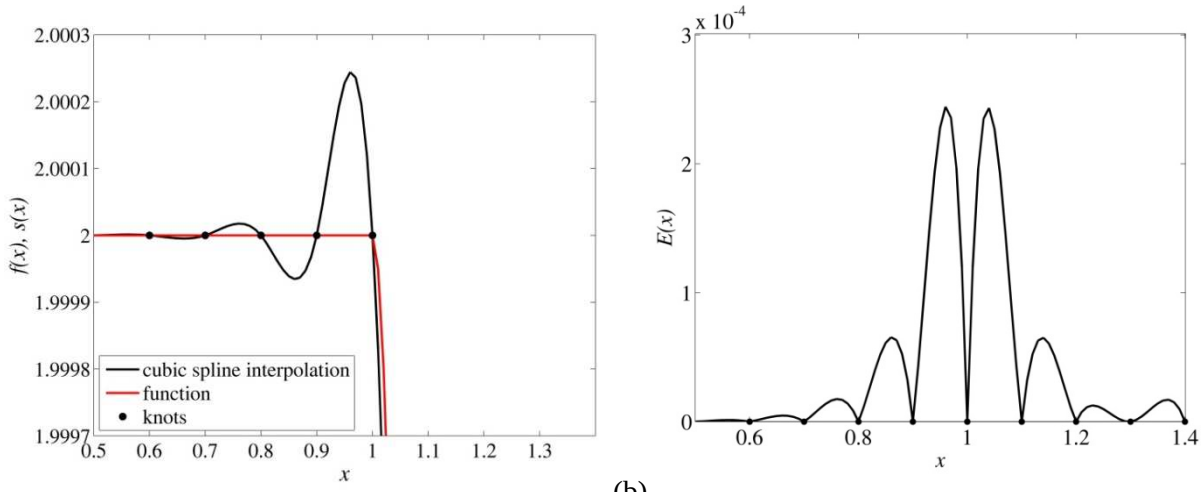

(a) (b)

Figure 2. Gibbs phenomenon of splines.

Due to the oscillations of the interpolating spline function around the discontinuity, the interpolation error:

$$E(x) = |f(x) - s(x)| \tag{4}$$

reaches the highest values in the two intervals at the sides of the discontinuity and gradually decreases with distance (see Figure 2b).The Interpolation Method for damage localization is based on turning this 'drawback' related to the Gibbs' phenomenon into a 'useful feature' to use as a sort of 'curvature discontinuity detector'.

Basing on all these observations, the increase of the interpolation error can be reasonably used in order to detect a localized increase of curvature. As shown in reference [7] a decrease of the interpolation error may correspond to a reduction of the discontinuity of curvature or may occur in the region between two very close discontinuities. The Interpolation Damage detection Method, as will be detailed in the following section, uses as a damage feature the interpolation error calculated for the Operational Deformed Shapes (ODS).

3. The Surface Interpolation Method

The basic idea of the Surface Interpolation Method can be described with reference to Figure 3. Let (x_0, y_0),…, (x_l, y_p),…, (x_{n_l+1}, y_{n_p+1}), be instrumented location of the plate where responses in terms of acceleration have been recorded. At each frequency value, the set of Frequency Response Functions (FRFs) H_R, calculated from measured responses, gives the operational deformed shape (ODS) at that frequency.

A localized reduction of stiffness at a certain location, causes a change of the operational shapes in the region close to that location hence this variation can be used to detect the location of damage. The change of the ODS between the undamaged and the damaged configurations can be highlighted by the interpolation of the ODSs through a smooth shape function and by the comparison between the interpolation errors related to the (possibly) damaged and the undamaged configurations. In the case of plate-like (that is bi-dimensional) structures, the interpolation of the operating deflection shapes can be carried out using bi-cubic spline functions.

Assuming that sensors lye on a rectangular grid $n_{l+1} \times n_{p+1}$, for each value of frequency f_i, the actual value $H_R(x_l, y_p)$ of the FRF at a given location (x_l, y_p), and its spline interpolation $H_S(x_l, y_p)$ must be known in order to calculate the value of the interpolation error at that location: $E(x_l, y_p)$, as shown in Figure 3. To this aim, the spline interpolation $H_S(x_l, y_p)$ is calculated assuming the FRFs at all the instrumented locations except $H_R(x_l, y_p)$.

Actually, if only one response is neglected in the interpolation, a non-regular grid is obtained. In order to overcome this problem, two regular grids have been defined, by neglecting all the responses recorded on one row or on one column of the grid.

Following the two-steps procedure outlined in section 2.1, at each instrumented location the two values of the bi-cubic spline interpolation (one for each of the two grids obtained removing one row or one column) can be calculated as:

$$H_{S,x}(x, y, f_i) = \sum_{i=0}^{3}\sum_{j=0}^{3} X_{jp,i(l-1)}(f_i)(x - x_{l-1})^i (y - y_p)^j \qquad x_l \in [x_{l-1}, x_{l+1}];\ y_p \in [y_p, y_{p+1}] \tag{5}$$

$$H_{S,y}(x, y, f_i) = \sum_{i=0}^{3}\sum_{j=0}^{3} Y_{j(p-1),il}(f_i)(x - x_{l-1})^i (y - y_{p-1})^j \qquad x_l \in [x_l, x_{l+1}];\ y_p \in [y_{p-1}, y_{p+1}] \tag{6}$$

For each frequency value f_i, the coefficients, $X_{jp,i(l-1)}$ and $Y_{j(p-1),il}$ are calculated as functions of the H_R measured at all the nodes of the grid except those with $x=x_l$ (for $X_{jp,i(l-1)}$) and except those with $y=y_p$ (for $Y_{j(p-1),il}$).

Considering the two values of the interpolated FRF, at each instrumented location (x_l, y_p) and for each frequency f_i, the value of the interpolation error at the given location can be calculated as:

$$E(x_l, y_p, f_i) = E_x(x_l, y_p, f_i) + E_y(x_l, y_p, f_i) \tag{7}$$

In order to characterize each location $P(x, y)$ (in the following the suffix p and l will be dropped for clarity of notation) with a single error parameter, the norm of the error on the significant frequency range (that is the frequency range with a signal to noise ratio sufficiently high to allow a correct definition of the FRF) is calculated:

$$E(x,y)=\sqrt{\sum_{i=n_o}^{n_o+N} E(x,y,f_i)^2} \tag{8}$$

The significant frequency range is selected limiting the summation in equation (8) to the frequency range of the fundamental modes of the structure that can be tuned basing on vibration tests carried out on the undamaged structure. In equation (8) N is the number of frequency lines in the Fourier transform correspondent to the frequency range starting at line n_o, where the signal to noise ratio is high enough to allow a correct definition of the FRFs.

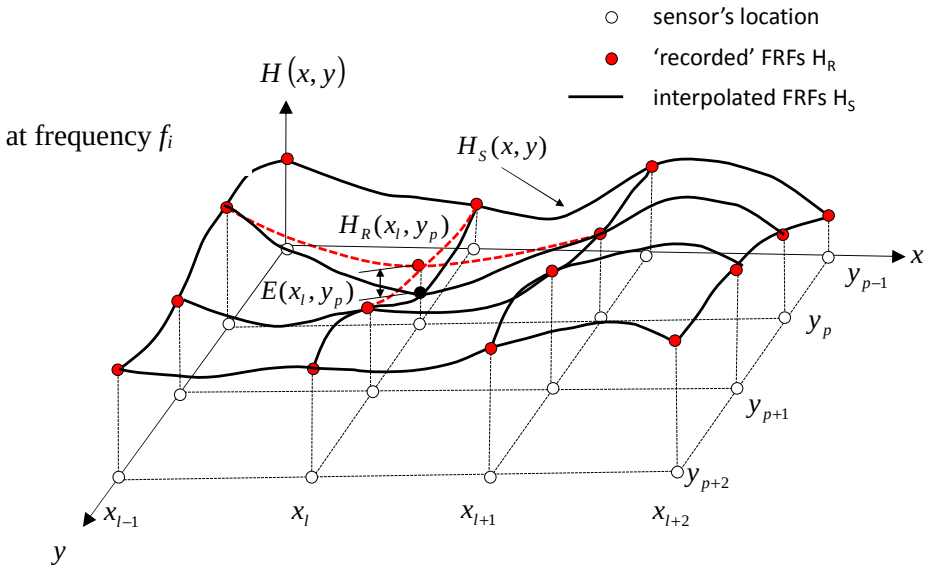

Figure 3. The interpolation error $E(x,y)$.

The values of the transfer functions H_R depend on the state of the structure. Hence, if the estimation of the error function through equation (8) is repeated in the baseline (undamaged) and in the inspection (possibly damaged) configuration, then the difference between the two values, denoted respectively by $E_o(x,y)$ and $E_d(x,y)$, can provide an indication about the existence of degradation at location (x, y):

$$\Delta E(x,y)=E_d(x,y)-E_0(x,y) \tag{9}$$

Due to the Gibbs phenomenon described in section 2.2, an increase in the interpolation error between the reference configuration and the current configuration at a station $P(x,y)$, i.e. $\Delta E(x,y)>0$, highlights a localized reduction of smoothness in the vibration amplitude profile.

A positive value of ΔE is thus assumed to be a symptom of a local decrease of stiffness at location $P(x,y)$ associated with the occurrence of damage. By this assumption, the following conditions are assumed to define the damage index $IDI(x, y)$:

$$\begin{aligned} IDI(x,y)&=\Delta E \quad && if \quad && \Delta E(x,y)\geq 0 \\ IDI(x,y)&=0 \quad && if \quad && \Delta E(x,y)<0 \end{aligned} \tag{10}$$

The first condition ($\Delta E>0$) corresponds to an increase of the interpolation error, that is to a decrease of the smoothness of the amplitude profile. On the contrary a decrease of the interpolation error, as shown in section 2.2, may be associated to an increase of smoothness or may occur in the region between two damaged sections due to an insufficient spatial sampling. In both cases it is not associated to a local reduction of stiffness hence a negative variation of the interpolation error will be assumed to correspond to a null value of the damage index.

Due to several sources, positive variations of the interpolation error E occur even if no damage is present. In order to remove the effect of these random variations, the statistical variation of this parameter can be studied and a threshold can be defined considering the tolerable value of the probability of false alarm P_f (see reference [6]). The threshold of ΔE can be estimated in terms of the average $\mu_{\Delta E}$

and the variance $\sigma_{\Delta E}$ of the values of ΔE at all the instrumented locations. Assuming a Normal distribution, the threshold ΔE_t can be defined as:

$$\Delta E_t(x,y) = \mu_{\Delta E} + \nu\sigma_{\Delta E} \tag{11}$$

The threshold can be fixed setting a value of the accepted probability of false alarm assuming the parameter ν as the quantile 1-P_f of the standard normal distribution.
The interpolation damage index (*IDI*) is then calculated as:

$$\begin{aligned} IDI(z) &= \Delta E(z) \quad if \quad \Delta E(z) \geq \Delta E_t(z) \\ IDI(z) &= 0 \quad if \quad \Delta E(z) < \Delta E_t(z) \end{aligned} \tag{12}$$

A localized decrease of stiffness causes a localized increase of curvature that, having in mind the discussion reported in section 2.2, corresponds to an increase of the interpolation error.

4. Experimental tests and results

3.1. Material and specimen

The plates were produced by poltrusion technique using E-glass fibres and vinylester matrix. The Heat Deflection Temperature (HDT) of the resin, measured by the producer, was 105°C. Fibre reinforcement consisted of three non-crimp fabrics. Each fabric had plies construction 0° / ± 45° and total areal weight of 600 g/m^2. The temperature in the heated mould was set to have 95% of the complete polymerization inside the mould.

	Elastic modulus [GPa]	Strength [MPa]
Traction 0°	27.5	437
Traction 90°	9.9	76
Bending 0°	20.6	551
Bending 90°	10.8	109

Table 1. Mechanical properties of the composite material.

The fibre volume fraction was almost 60%. Some mechanical properties of the composite were measured according to international standards (ISO 527 and ISO 14125 for tensile and bending test, respectively). The average results are listed in Table 1.
Specimens for testing were square plates with average thickness of ≈8 mm and sides of ≈500 mm.

3.2. Impact hammer tests

The plate was suspended with a bungee cord to approximate free-free boundary conditions and subjected to a pulse load applied to each of the intersections of a grid depicted on the specimen (see **Figure 4**).

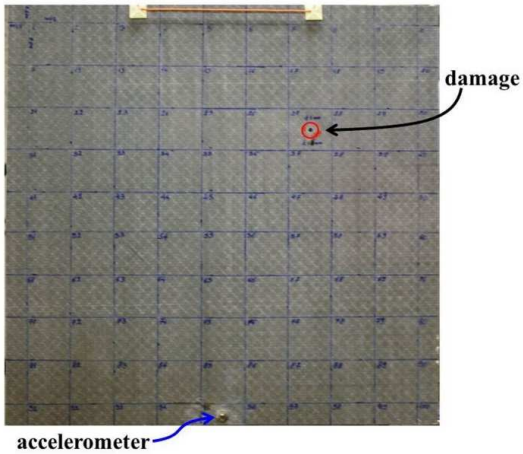

Figure 4. Grid for pulse load application and position of the accelerometer and damage.

The load is applied by an impulse hammer Dytran 5801A5 equipped with a load cell of 4.45 kN. A piezoelectric accelerometer Bruel&Kiaer 4384, fixed at the reference location shown in Figure 4 (middle of the plate close to the lower edge) was used to measure acceleration. Data were recorded with an acquisition system National Instruments 9234, 24 bit resolution and maximum sample rate of 51200 Hz. For each pulse load, 51200 measurements were stored. The Frequency Response Functions between each grid point and the reference one were determined from three impacts at each point and, in order to reduce the random fluctuations in their estimation, three FRFs were averaged at each point. The plate was tested before (as reference) and after a damage simulating a manufacturing flaw. The imparted damage was of cylindrical shape 5 mm diameter and half thickness depth. The red circle in Figure 4 is shows the position of the damage.

3.3. Results

The Operational Deformed Shapes are contained in each row or column of the FRF matrix that can be calculated in terms of receptances (ratio between acceleration and force). In this case, the receptances at each node p (p=1, 2… 100) were calculated as the ratio between $R_q(\omega)$, the FFT of the acceleration recorded at the location q (see **Figure 4**) and $F_p(\omega)$, the FFT of the force impacted by the hammer at node p:

$$H_p(\omega) = \frac{R_q(\omega)}{F_p(\omega)} \tag{13}$$

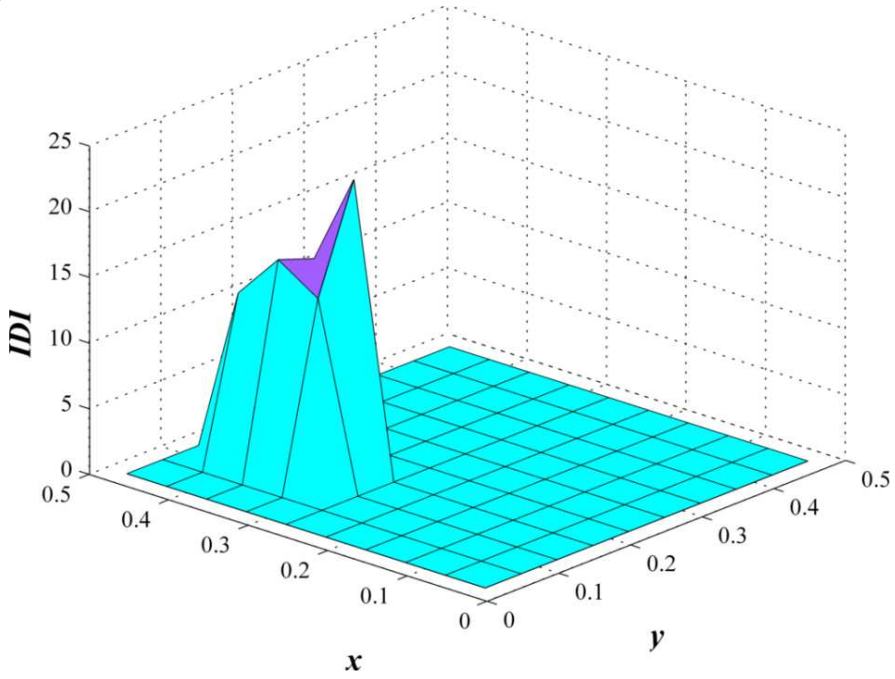

Figure 5. Results for the damage induced in the composite plate

For example, the function $H_{55}(\omega)$ was obtained by impacting the beam at point 55 and measuring the response at the location of the accelerometer.

For the application of the SIM, the probability of false alarm has been assumed equal to 2% (ν=2 in equation 11) and the frequency range for the application of the SIM, assuming the FRF measured in the undamaged configuration, was set as 40-800 Hz (n_o= 40, N=800 in equation 8).

In Figure 5 the results of the application of the SIM are reported showing that the damaged location is correctly detected by the algorithm. It is noted that the damage index exhibits the highest values at the four nodes of the damaged elements even if high values are found also at the adjacent locations. This is due, as explained in reference [5], to the interpolation process that somehow spreads the reduction of

the accuracy in the interpolation to the locations close to the one where the reduction of smoothness occurs. In any case, this phenomenon occurs only in the vicinity of the effectively damaged area, even if it can reduce the precision in the identification of the contour of the damaged area, it does not hamper the correct localization.

5. Conclusions

In this paper are summarized the results of the application of the Surface Interpolation Method (SIM) to the case of a damaged glass fiber composite plate in order to experimentally verify the feasibility application of the proposed algorithm. Results indicate that the method is a viable method for damage localization providing, with respect to other method proposed in literature, the same accuracy in damage localization with at a lower computational effort. Advances in sensors technology and miniaturized signal processing platforms allow exploring the possibility of realizing an autonomous monitoring system based on responses recorded by a large number of sensors widely distributed over the structure. From this point of view the minimum interaction with a human operator required by the SIM makes it appealing for automatic damage detection through a permanent monitoring system integrated with data processing software.

Acknowledgments

The present work was partially supported by the ReLuis-DPC Executive Project 2014-2016, Special Project “Monitoring”, whose contribution is gratefully acknowledged.

References

[1] Fan W, Qiao P 2011 Vibration-based Damage Identification Methods: A Review and Comparative Study *Structural Health Monitoring* **10**(1) p. 83–29
[2] Ratcliffe CP 2000 A frequency and curvature based experimental method for locating damage in structures. *Transactions of the American Society of Mechanical Engineers. Journal of Vibration and Acoustics*, **122**: 324–329
[3] Sampaio R P C , Maia N M M Silva J M M 1999 Damage detection using the frequency response function curvature method. *Journal of Sound and Vibration*, **226(**5) p. 1029 1042
[4] Limongelli M P 2010 Frequency Response Function Interpolation for Damage Detection under Changing Environment. *Mechanical Systems and Signal Processing* **24**(8), p. 2898-2913
[5] Limongelli M P 2011 The interpolation damage detection method for frames under seismic excitation. *Journal of Sound and Vibration*, **330** p.5474–5489
[6] Limongelli M P 2014 Seismic health monitoring of an instrumented multistorey building using the Interpolation Method *Earthquake Engng. Struct. Dyn*. **43**(11) p.1581-1602
[7] Zhan Z, Martin C F 1997 Convergence and Gibbs' phenomenon in cubic spline interpolation of discontinuous functions *Journal of Computational and Applied Mathematics* **87** p. 359-371